Heliyon 8 (2022) e10936

Contents lists available at ScienceDirect

Heliyon

journal homepage: www.cell.com/heliyon

Research article

Rational synthesis and characterization of highly water stable MOF@GO composite for efficient removal of mercury (Hg^{2+}) from water☆

Ahmed M. Fallatah [a,1], Habib Ur Rehman Shah [b,c,*,1], Khalil Ahmad [b,f,***,1], Muhammad Ashfaq [b,**], Abdul Rauf [b], Muhammad Muneer [d], Mohamed M. Ibrahim [a], Zeinhom M. El-Bahy [e], Amir Shahzad [b], Afshain Babras [b]

[a] Department of Chemistry, College of Science, Taif University, PO Box 11099, Taif 21944, Saudi Arabia
[b] Institute of Chemistry, Baghdad Ul Jadeed Campus, The Islamia University of Bahawapur-63100, Punjab, Pakistan
[c] Roy & Diana Vagelos Laboratories, Department of Chemistry, University of Pennsylvania, Philadelphia, PA 19104-6323, United States
[d] Department of Chemistry, Khwaja Fareed University of Engineering and Information Technology Rahimyarkhan-64200, Punjab, Pakistan
[e] Department of Chemistry, Faculty of Science, Al-Azhar University, Nasr City 11884, Cairo, Egypt
[f] Department of Chemistry, University of Management and Technology Sialkot Campus Sialkot, Punjab, Pakistan

GRAPHICAL ABSTRACT

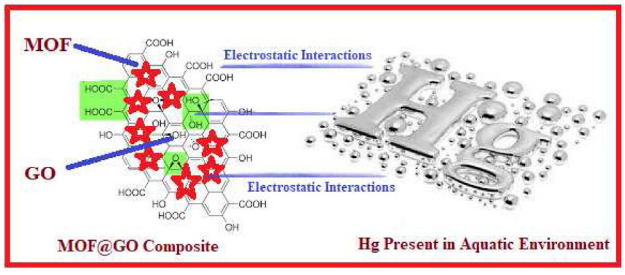

ARTICLE INFO

Keywords:
Metal organic frameworks
Graphene oxide
Adsorption
Freundlich model
Langmuir model
Powdered X-ray diffraction

ABSTRACT

The present study is aimed at adsorptive removal of Mercury (Hg^{2+}) using highly functionalized nanomaterials based on Graphene Oxide Zeolitic Imidazolate Framework composite (ZIF-67@GO). Solvothermal methodology was used to synthesize ZIF-67@GO composite. Synthesized compounds were confirmed by FTIR, SEM, PXRD and EDX analysis. The as-prepared ZIF-67@GO was tested as efficient adsorbent for effective removal of Mercury (Hg^{2+}) from aquatic environment. The atomic adsorption spectrophotometer was used to monitor the process of adsorption of Hg^{+2} on ZIF-67@GO. From the adsorption data, the maximum removal efficiency achieved was 91.1% using 10 mg amount of composite for 50 mL using 20 ppm Mercury (Hg^{2+}) solution. Different parameters like pH, contact time, concentration, adsorption kinetics and isotherm were also examined to explore adsorption process. Adsorption data fitted well for Freundlich Model having R^2 value of 0.9925 than Langmuir Isotherm with R^2 value of 0.9238. Kinetics were rapid and excellently described via 2nd order model with $R^2 = 0.99946$ than 1st order model with R^2 value of 0.8836. Freundlich and pseudo 2nd order models validated that multilayer

☆ This article is dedicated to my dear colleagues, Dr Khalil Ahmad on Joining UMT Sialkot as Assistant Professor, Dr M. Aadil Khan and Dr Safdar Hussain on Joining IUB RYK campus as Lecturer Chemistry.

* Corresponding author.
** Corresponding author.
*** Corresponding author.
E-mail addresses: habibshah26@gmail.com (H.U.R. Shah), khalilnoorpur@gmail.com (K. Ahmad), chashfaqiub@yahoo.com (M. Ashfaq).

[1] Have equal contribution.

https://doi.org/10.1016/j.heliyon.2022.e10936
Received 11 May 2022; Received in revised form 25 July 2022; Accepted 29 September 2022

chemisorption occurs during adsorption process due to the presence of highly functionalized sites on ZIF-67@GO composite. The synthesized composite material has shown excellent reusability. Thus, water stable ZIF-67@GO composites can efficiently be used for Mercury (Hg^{2+}) confiscation from water.

1. Introduction

Water is key to maintain life on the earth. It is necessary to have sufficient amount of drinking clean water to ensure safety to human health. According to international law, access to clean water is the basic human right. Now a days, the availability of clean drinking water is difficult due to water pollution. Both natural and anthropogenic activities are responsible for water pollution. Recently, water pollution has become a serious threats to human beings. According to latest reports, 8 million human beings died every year due to water borne diseases [1]. According to United Nation Agenda 2030, food contamination due to water pollution is one of the most serious global issues which should be resolved as soon as possible [2]. The extensive water solubility of contaminants is responsible for food contamination. The main objective of sustainable development is the frequent access for clean drinking water for everyone [3]. Among water pollutants, heavy metal ions are the emerging water pollutants due to their severe toxicity, persistence, water mobility and accumulation tendency [4]. Heavy metal traces are abundantly found in both sediment and water [5]. Among all heavy metals traces, Mercury (Hg) is volatile and has persistency and therefore can easily transform into other toxic forms leading to bioaccumulation. The "Hg" was the chemical symbol given to mercury which was meaning liquid silver [6]. Environmental Protection Agency (EPA) limited inorganic mercury level up to 144 ppm. EPA suggests that adult with average weight can expose themselves to 0.021 mg of organic or inorganic mercury every day in water or food without any harm. While the Food and Drug Administration (FDA) limited maximum mercury level of 2 ppb in bottled water. The National Institute for Occupation Safety and Health Administration known as OSHA prescribed the minimum limit of 1.2 ppb for organic mercury, 6.1 ppb of inorganic mercury vapors in the air of a workroom for 10 h shift [7, 8].

The main sources responsible for Hg contamination include, agricultural material, mining discharge, atmospheric deposition, chemical industries, landfills, military sites, mines and metal processing industries [9]. The global ocean contamination by mercury is due to deposit in shallow sediments [10]. The lands connections with estuaries, oceans are responsible for terrestrial Hg transport to oceans. Usually, the mass balance model gives quantitative information about transport and sources of contaminants. For example, Chesapeake Bay and Long Island Sound (LIS), estimates the removal of sedimentary Hg [11, 12, 13, 14]. It is observed that Hg contamination increases ten times since start of rapid industrial revolution [15, 16]. Mercury exists in the form either methyl-mercury or elemental-mercury. Mercury in any of these mentioned forms is toxic and effects on both central nervous system (CNS) and peripheral nervous system (PNS) [17, 18]. The intrusion of trace amount of mercury vapors effects digestive, nervous, lungs, kidney and immune systems. Salts of mercury are toxic to eyes, kidneys, gastrointestinal tract and skin and may be fatal if ingested even in very small amount [19]. Sometimes mercury dermal or ingestion exposure results in behavioral and neurological disorders which results in insomnia, tremors, memory loss, headaches, motor and cognitive dysfunctions and neuromuscular effects with a minimum concentration of 20 $\mu g/m^3$ (in the air) [20]. A significant example regarding mercury exposure effecting human health was observed during 1932–1968 in Minamata, Japan where an acetic acid producing factory wasted its effluent directly into a bay. This bay was supposed to be rich in shellfish and fish providing livelihood for fishermen and local residents. Fishes were contaminated and about 50,000 peoples were seriously affected and 2000 among them were certified dead [21, 22].

Due to hazardous nature of mercury, its confiscation is necessary. The different methods were adopted in the past for the confiscation of heavy metal ions from water but these methods have some disadvantages as well. Some of the methods based on the advanced oxidation (AOP) and adsorption processes using porous materials [11, 23, 24, 25, 26, 27]. These utilized methods exhibited various shortcomings like, high cost, complex procedure, low efficiency, less selectivity and reusability [28, 29, 30, 31]. To date, four processes have been used for the removal of mercury. These methods suffer some limitations as well. These methods along with their limitations are; **1st** by filtration/coagulation (using $AlSO_4$ which precipitates out Hg from water has detection limitation), **2nd** by activated carbon (remove Hg by adsorption process has limitation because effectiveness depends upon Hg concentration), **3rd** by reverse osmosis (by passing water through semi-permeable poly-amide membrane has limitation that this membrane is very expensive) and **4th** by lime softening (using $Ca(OH)_2$ to precipitate out the heavy metal ions from water) [32, 33, 34, 35, 36, 37, 38, 39, 40].

Recently, a new and versatile class of porous coordination polymers, known as Metal Organic Frameworks (**MOFs**) and their derived composites have shown promising capabilities for removing emerging environmental pollutants. Their versatility can be accessed from their high water and thermal stability as well as broad range of applications [41, 42, 43, 44, 45, 46]. High water solubility of emerging pollutants is serious in their confiscation as most of the compounds prepared for the purpose are water soluble themselves. Therefore, MOFs are prominent candidates for effective removal of emerging pollutants especially heavy metals. MOFs and their composites have shown excellent adsorption capacities for different heavy metals especially Hg^{2+} [47].

From all reported MOFs based functionalized materials for adsorptive removal of heavy metals, one special kind MOFs named as ZIFs (zeolitic imidazolate frameworks) have given favorable adsorption performances for removal of emerging pollutants like heavy metals and organic pollutants due to higher surface areas, thermal and water stabilities [48, 49, 50]. The development of a cost effective, convenient and facile method of preparation to get modified Zeolitic imidazolate frameworks is necessary for the effective removal of Hg^{2+} from water [51]. For improving adsorption performance, the adsorbent surfaces must be functionalized using different methodologies. Various studies successfully explored the modified materials based on composites of MOFs and graphene oxide. ZIFs have great efficiency for pollutants removal from water when its composite is made with graphene oxide. This functionalized material have been efficiently utilized for confiscation of emerging pollutants including organic and inorganic from water [52, 53]. These outcomes indicated that the graphene oxide and ZIFs composites have higher water and thermal stabilities as compared to simple ZIFs [54]. As per literature, few reports are available on utilization of MOFs based functionalized material composites for confiscation of Hg^{2+} from water. A few reports are summarized in Table 1. Therefore, this study aimed at the synthesis of graphene oxide zeolitic imidazolate metal organic frameworks composites using solvothermal methodology and was applied to examine the adsorption capability of as-synthesized composite for removal of Hg^{2+}. We proposed that this study will facilitate young researchers to explore their vision in developing strategies for removal of toxic pollutants from aquatic environment.

2. Materials and methods

2.1. Materials used

Hydrochloric acid, Sodium hydroxide, sulphuric acid, 2-methyl imidazole, Graphite powder, cobalt nitrate hexahydrate, potassium permanganate and methanol were of analytical grade and purchased from SIGMA-ALDRICH, Steinhem, Switzerland.

Table 1. Maximum adsorption capacities of various adsorbents for mercury (Hg^{2+}) removal from water.

Sr No.	Adsorbent Used	q_{max} (mg/g)	Refs.
1	ACFs-SH	11–15	[60]
2	Ox-MAC and SH-MAC	35.4	[61]
3	MWCNTs	84.66	[62]
4	2-MBTZ-Fe_3O_4	98.6	[63]
5	Sulfurized MAC	38.3	[64]
6	GG-cl-CH = N–$(CH_2)_6$–N=CH-GG	41.13	[65]
7	POSS-SH	12.90	[66]
8	AL-SH	101.2	[67]
9	ALP	107.5	[68]
10	Polypyrrole-CTs	40	[69]
11	Sulfur-functionalized silica	47.50	[70]
12	BTESPT-SGs	93.32	[71]
13	ATP-APTES	90	[72]
14	ZIF-67@GO	131.07	This Study

2.2. Methods

2.2.1. Method for preparation of GO

Graphene Oxide (GO) was synthesized using 1 g graphite powder by using Hummer's method. Practically, 1 g of graphite (powder) having size <20 μm was taken in 250 Ml. About 23 mL of sulphuric acid (H_2SO_4) was mixed dropwise into system which was maintained at 0–5 °C under vigorous stirring. About 3 g of $KMnO_4$ was mixed very slowly into mixture under vigorous stirring. The mixture obtained was then shifted to a fixed temperature (40 °C) maintained in oil bath with vigorous stirring for 30 min. After that 50 mL of distilled H_2O added and temperature was increased from 40 to 90 °C. The solution was maintained on stirring for half an hour. After that 150 mL of distilled H_2O and 6 mL of 30% H_2O_2 added to stirring mixture. This addition will result in the color change which leads to foundation of yellowish solution. Resulting solution was left over for some time for decanting obtained product. The obtained solution was washed many times with a mixture of HCl/H_2O to eliminate lasting metal ions. Solution obtained then decanted and solution over decanted material was removed. Resultant product obtained then desiccated in oven at 70 °C for 12 h. The dried product was added with a 300 mL distilled H_2O and solution mixture obtained, stirred overnight at ambient temperature. Obtained suspension was sonicated and centrifuged at 6000 rpm for 20 min. The resultant mixture was filtered and dried at 60 °C for 24 h in an oven [55].

2.2.2. Method for the preparation of the composite (ZIF-67@GO)

For ZIF-67@GO synthesis, a 20 mg graphene oxide (GO) was dispersed in 10 mL distilled water (H_2O). Obtained solution was stirred for 10 min to obtain homogenous GO suspension and sonicated for 40 min. Suspension obtained was mixed with solution containing 3 mmol of cobalt salt ($Co(NO_3)_2.6H_2O$) solution in 10 mL water. Another solution was made by dissolving 2-methyl imidazole (2-MIM) in appropriate amount of water [56]. Solution containing cobalt salt and GO were mixed dropwise in 2-methyl imidazole. Mixture obtained was kept on stirred for 1 h at room temperature. The resulting solution was left overnight for aging and centrifuged at 6000 rpm for 20 min. The product obtained washed with a solution containing CH_3OH & H_2O in 6:4 ratio, several times, to remove unwanted materials. Produced solid product was dried in oven at 80 °C for 12 h [38]. The resultant functionalized nanomaterial was used further to study the adsorption of mercury (Hg^{+2}) from water.

2.3. Characterizations

The FTIR analysis of MOFs and composites (ZIF-67@GO) were carried out via ATR technique in 4000–400 cm^{-1} range using TENSOR-27 (model Bruker-2010) spectrometer. The *p*H was obtained using SUP-pH6, pH meter. Absorption analyses were recorded by Atomic Absorption Spectrometer (AAS) (Perkin Elmer Analyst-100) at wavelength of 253 nm wavelength. The SEM (Scanning-Electron-Microscopy) was carried out using Quanta-250 equipped with EDX scanner. The PXRD (Powder X-ray (XD-3)) were used to check morphologies of prepared MOF and ZIF-67@GO.

2.4. Adsorption experiment

Adsorption experiment was carried out using 10 mg amount of adsorbent was added in each solution containing (50 mL) having concentration range of 10–20 ppm. Contact time was 90 min and pH were adjusted by using 0.1 M HCl and NaOH respectively. Adjusted pH was used for the analysis of each and every sample. Initial concentration of 10, 15 and 20 ppm were used with specific adsorbent dose. After performing adsorption experiment, it was found that adsorption process was fast and attained equilibrium after 90 min. This time of 90 min used as equilibrium time. After adsorption experiment, the initial and final concentrations were measured using Atomic Absorption Spectrometer (AAS) [38].

From results obtained from standard solutions, the observed data was applied to calculate the removal efficiency and adsorption-capacity of ZIF-67@GO for Hg^{+2} removal using Eqs. (1) and (2) [57,58]. Moreover, the different parameters effecting adsorption like, pH, contact time, concentration, pseudo 1st and 2nd order, Freundlich and Langmuir model were also studied to explain overall adsorption process.

$$q = \frac{(Co - Ce\ )\ V}{m} \tag{1}$$

$$R = \frac{(Co - Ce)}{Ce} \times 100 \tag{2}$$

where.

C_e = Equilibrium concentration of Hg^{2+} (mg/L)
R = Removal efficiency
C° = Original Hg^{+2} concentration (mg/L)
q = Adsorption capacity (mg/g)
m = amount of adsorbent V = Volume-of Solution of Hg^{2+}

The kinetic models i.e., Pseudo 1st and 2nd order applied and value for adsorption capacities were calculated using Eqs. (3) and (4) respectively.

$$K_1 = \frac{\ln qe - \ln(qe - qt)}{t} \tag{3}$$

$$K_2 = \frac{qt}{t}\left(1 / qe^2 + 1 / qe\right) \tag{4}$$

qe = Adsorption-Capacity (mg/g),
q_t is Adsorption-Capacity (mg/g),
t is Adsorption-Time (h),
K_1 is Pseudo-first-Order Adsorption Rate Constant (h^{-1}),
K_2 is the Adsorption-Rate-Constant of Pseudo-Second-Order (gm g^{-1} h^{-1}).

2.5. Determination of point of zero charge

The salt addition method was used to determine the point of zero charge of ZIF-67@GO. The 20 mL solution was taken and initial pH of 0.10 mol/L NaCl was maintained at different pH like 2, 4, 6, 8, and 10 using 0.1 mol/L NaOH and 0.1 mol/L HCl in five different conical flasks. After that, 20 mg of ZIF-67@GO added to each conical flask. The resulting solution mixtures were shaken for 24 h at 25 °C. The resulting

mixtures were filtered off and final pH of the solution was determined. The pH difference was calculated and plotted against initial pH. When the change in pH is zero then initial pH is equal to point of zero charge that was calculated as 4.8 in case of newly prepared ZIF-67@GO composite (Figure S7) [59]. The ZIF-67@GO composite was positively charged below pH 4.2 (highly acidic media) therefore Hg^{+2} adsorption was inhibited on composite due to H^{+} ions interferences.

3. Results and discussion

The MOF and the MOF@GO composites were successfully synthesized by following solvothermal method of synthesis. By this method the MOF (ZIF-67) was efficiently grown on the surface of graphene oxide (GO) (Figure 1). After synthesis the materials were subjected to different characterizations in order to check the confirmation of synthesis. First of all, the SEM analysis of MOF and MOF@GO composites were carried out and the results unveiled that ZIF-67 has cubic morphology while the composites SEM showed efficient growth of ZIF-67 on the surface of GO. Figure 2a–2f representing SEM images and it can be established that MOF and MOF@GO composite was successfully synthesized (Figure 2b, 2d). It was observed that, during synthesis, the GO act like surfactant leading to the MOF@GO composite size reduction. After that, the prepared MOF@GO composite was subjected to EDX analysis, the results indicated the elemental composition having following % of 18.95, 15.68, 25.24, 10.3 of C, N, O and Co respectively. While the XRD results revealed the diffraction peaks of MOF of ZIF-67 at 2θ value of 7.0°, 10.33°, 12.8°, 14.64°, 16.4° and 17.98° (Figure S2). On the other hand, GO was analyzed through XRD technique which confirmed the diffraction peak at 2θ value of 11.1° 25.5° respectively. The diffraction peak at 2θ value of 11.1° showed the presence of oxygen containing groups on the surface of graphite while other important peaks at 16.4°, 18.2°, 22.2°, 25.5° and 32.3° values and were in accordance with reported literature (Figure S3). The obtained results were subjected to further analysis and it was confirmed that GO having interlayer spacing of 0.74 nm interlayer spacing (obtained from Braggs law using Origin software). Besides, GO peaks were not observed in MOF@GO composites indicating complete exfoliation of GO, full communication and uniform dispersion of GO with assemblies of ZIF-67. The FTIR study was carried out to know GO structural features (Figure S4) that approves the C–C, C–O and C–O–C peaks at about 1540.98 cm^{-1}, 1021.73 cm^{-1} correspondingly. While oxygenated groups peaks were reduced because of the GO reduction into rGO in solvothermal synthesis method. The FTIR results for ZIF-67 & its composite (ZIF-67@GO) confirmed synthesis by presence of signal (peak) on 1421.21 cm^{-1} & 1557.13 cm^{-1} correspondingly (Figures S5, S6). Furthermore, to check the adsorptive removal of Hg^{+2} ions, the EDX analysis of ZIF-67@GO composites were also performed before and after the adsorption process. From EDX it is clear that Hg^{+2} ions are successfully adsorbed from water (Figure S7). The factors effecting adsorption process were also examined to have removal efficiency and adsorption capacity of prepared ZIF-67@GO composite. After study it was established that contact time established on 90 min and the 131.07 mg/g adsorption capacity obtained with 91.1 % removal efficiency.

4. Factors that affect Hg^{+2} adsorption

4.1. The Hg^{2+} concentration effect on adsorption

During adsorption process the effect of Hg^{2+} concentration was checked and it was observed that as the concentration of Hg^{2+} increased from 10 to 30 mg/L then the adsorption capacity value also increased from 95.66 to 131.07 mg/L. This relationship is shown in Figure 3. This whole may be due to the fact that the higher concentration of Hg^{2+} which resulted in greater mass transfer between the liquid and solid phase. The Hg^{2+} removal efficiency reduced from 91.1 % to 59.9 % value by increasing Hg^{2+} amount. The happened due to insufficient availability of active sites of adsorbents or may be due to the active site which got hold on excess in concentration.

4.2. Effect of pH

After knowing concentration effect, the effect of pH on the removal efficiency and adsorption capacity was checked (Figure 4). The highest value 91.1% for removal efficiency was achieved at neutral pH (7.0 ± 1). The presence of various functional group on GO that persist negative charge in pH range of 2–11. So, removal efficiency value surges with pH from acidic pH due to electrostatic interactions between the negatively

Figure 1. Schematic Representation of The Synthesis of Zeolitic Imidazolate Framework (ZIF-67) And Graphene Oxide Metal Organic Framework Composite (ZIF-67@GO) by solvothermal Methodology.

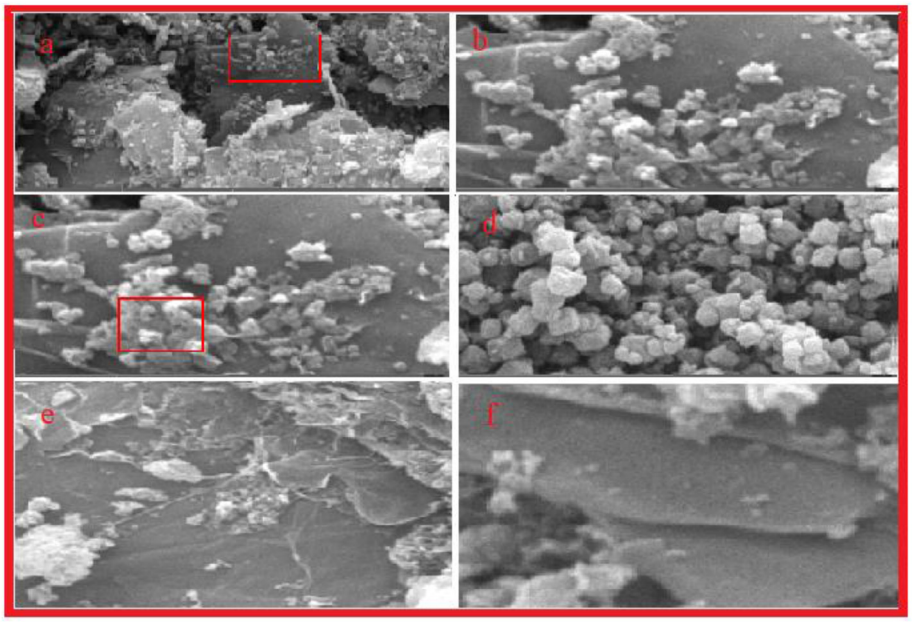

Figure 2. SEM analysis of ZIF-67@GO composite (a,b,c) at 10 μm respectively (b,c) at 2 μm confirming the growth of ZIF-67 on GO sheets and Figure (d) showing the ZIF-67 cubes formation on fine GO sheets at 100 nm (e, f) shows SEM of GO at 5 and 2 μm.

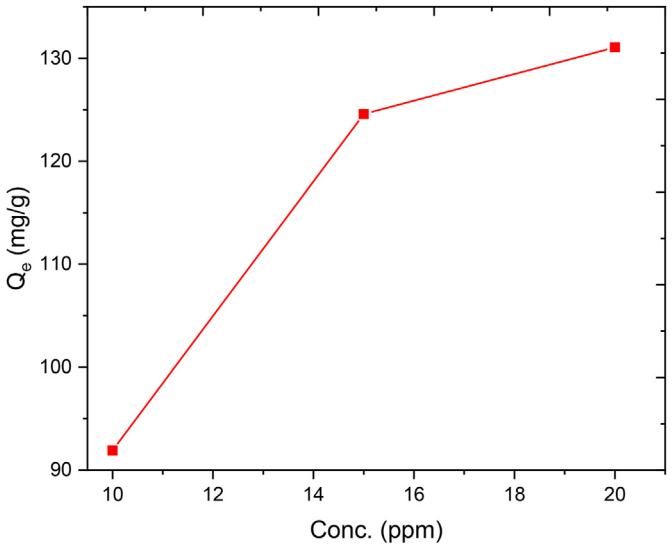

Figure 3. Adsorption capacity with respect to concentration of metal ion (Hg^{2+}), it is clear from the graph that adsorption capacity increases with time and maximum adsorption capacity of ZIF-67@GO achieved at 20 ppm concentration.

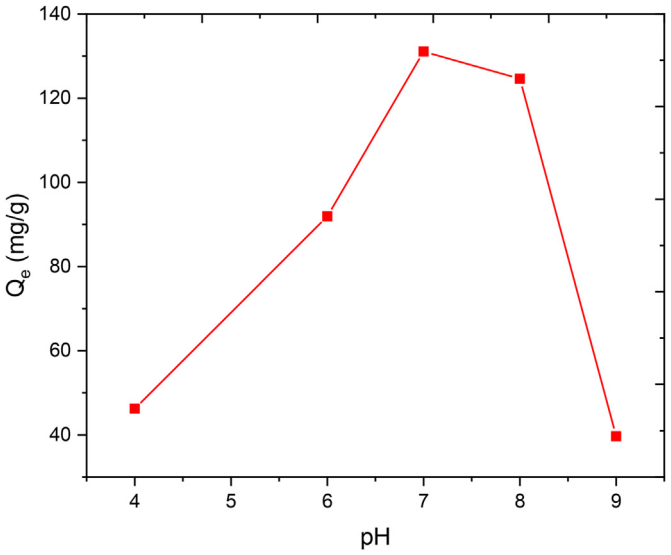

Figure 4. Adsorption capacity with respect to pH, it can clearly be observed that the maximum adsorption capacity was achieved at neutral pH.

charged composite and positively charged metal ion Hg^{2+}. While at higher pH metal (Hg^{2+}) still occur in positive form causing repulsion with appropriate parts of MOF@GO composite which resulted in decrease in the removal efficiency from 91% to 59%. This is because the prepared composite has shown removal efficiency at neutral pH. On the basis of results obtained, the pH was efficiently adjusted at 7.0 ± 1 for accompanying study of Hg^{2+} by ZIF-67@GO composite.

4.3. Contact time

The effect of contact time was also noticed for Hg^{+2} adsorption on ZIF-67@GO surface. The results of effect of time on adsorption capacity and removal efficiency are indicated in Figure 5a and 5b. It was observed from the results that the value of adsorption capacity increases after 80 min time span and became maximum at 90 min. This was demonstrated as the equilibrium, after that time the adsorption capacity tend to decreases. The increase was due to quick diffusion of metal ions from aqueous solution by ZIF-67@GO composite. End results clearly showed that when the contact time increases the sites availability will also increases and after equilibrium the adsorption decreases due to the metal attachments decrease. The maximum value of adsorption capacity on time of equilibrium obtained as high as 131.07 mg g^{-1} from aqueous media having 20 ppm Hg^{2+} concentration using 10 mg adsorbents.

5. Interpretation of physical models

5.1. Adsorption kinetics

The Hg^{2+} adsorption by ZIF-67@GO composite examined by different kinetics for example, pseudo 1st and 2nd order model (Figure 6a and 6b).

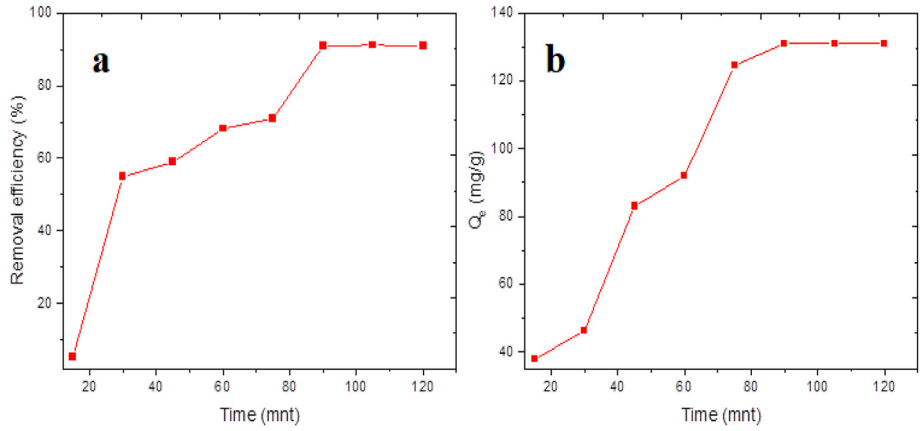

Figure 5. Removal Efficiency with time, it can easily be seen that the maximum removal efficiency was achieved at 90 min which is its equilibrium time (a) Adsorption Capacity With respect to Time (b).

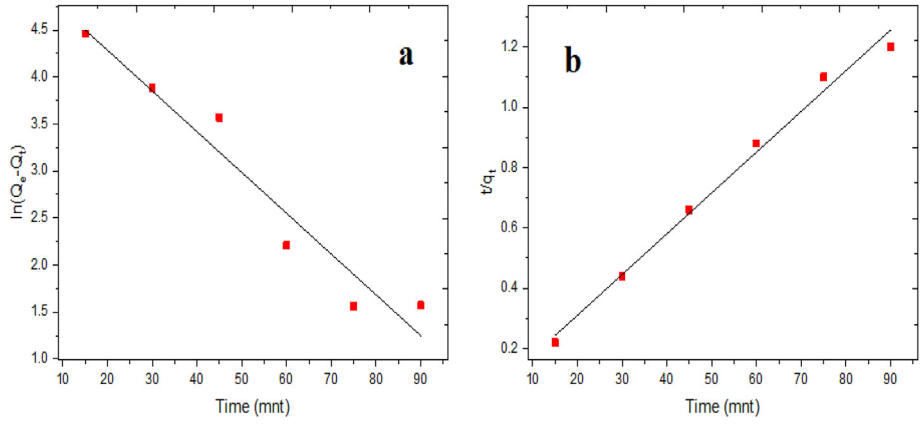

Figure 6. Pseudo 1st data not fitted well (a) and 2nd Order which is best fitted in this case (b).

Table 2. Kinetic parameters for pseudo 1st and 2nd order models for MG removal from water using ZIF-67@GO composites.

Adsorbent Used	Pseudo 1st order Model			Pseudo 2nd Order Model		
	Intercept	Slope	R^2	Intercept	Slope	R^2
ZIF-67@GO	5.4288	-0.03029	0.8836	0.17166	0.00227	0.99946

R^2 = Linear correlation coefficient.

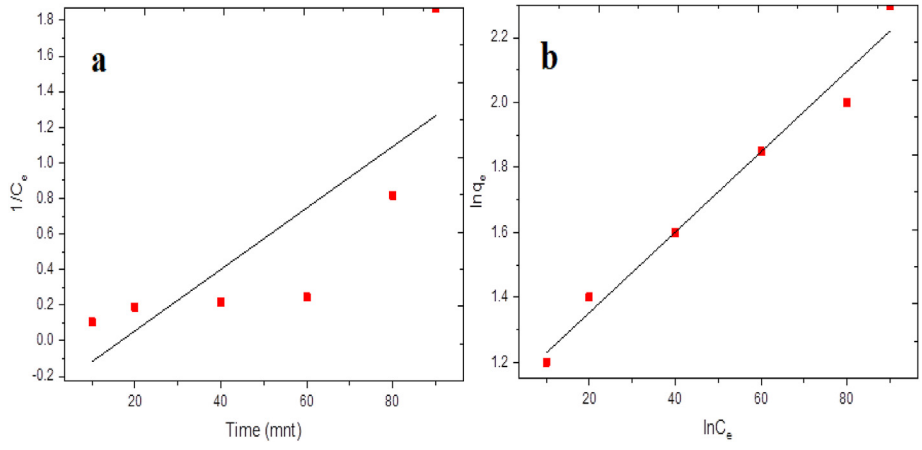

Figure 7. Langmuir Model is not fitted well (a) Freundlich Model was fitted well (b).

Table 3. Isothermal parameters for Langmuir and Freundlich model.

Adsorbent Used	Langmuir Model			Freundlich Model		
	Intercept	Slope	R^2	Intercept	Slope	R^2
ZIF-67@GO	0.0089	-0.00371	0.92385	1.51607	0.57627	0.9925

R^2 = Linear correlation coefficient.

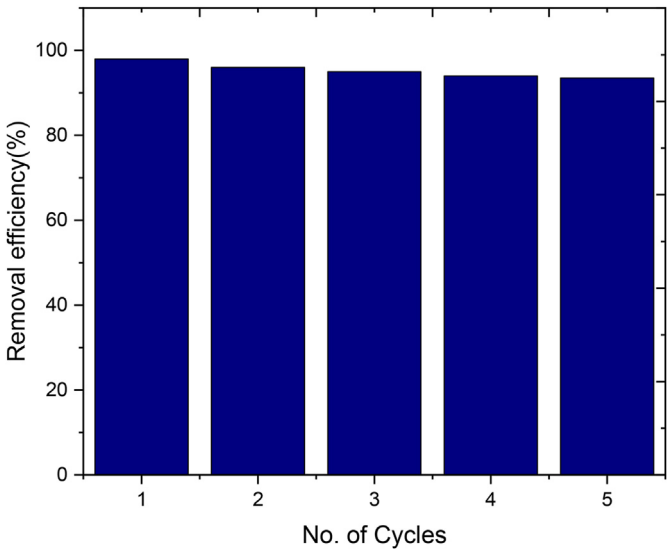

Figure 8. Regeneration studies of adsorbent, results showed that prepared composite showed excellent reusability and removal efficiency was not decreased marginally

The value of R^2 (correlation coefficients) for kinetic models were successfully calculated. The results indicated that correlation coefficient value of 0.9995 for the 2nd order model showed this model was best fitted for the Hg^{2+} adsorption using ZIF-67@GO composite. This showed that chemisorption process involved in determining rate of reaction. This also showed adsorption process occurs because of forces which formed of exchange or sharing of electrons between polar-group like amines and some other metal ions. Results shown in Figure 6b and 6b and are calculations are described in Table 2.

5.2. Adsorption isotherm

For study of isotherm, the different models like, Freundlich and Langmuir model were applied to have clear adsorption isotherm for Hg^{2+} adsorption by using ZIF-67@GO. The results of adsorption-isotherm studies are given in Figure 7a, 7b, Table 3. Results showed that R^2 (correspondence correlation coefficient) value for Langmuir-model showed excellent results as compared to Freundlich model. Therefore, Freundlich model (adsorption isotherm having value of 131.07 mg g^{-1} adsorption capacity) was best suited for explaining the adsorption of metal ion by using the prepared composite (ZIF-67@GO).

5.3. Regeneration of adsorbent

The regeneration experiment for the used adsorbent were performed that is important characteristic of MOFs adsorbents which make them superior to the other adsorbent used for the adsorption. For regeneration studies, the mixture of ethanol/HCl in ratios 1:9 utilized as model (standard) desorbing-agents. Subsequently, after regeneration of already used adsorbent, the value of removal efficiency calculated and it was observed that it reduces from 91.1% to 89.9% showing higher reusability even after couple of recycle experiments. These consequences indicated that ZIF-67@GO has shown exceptional removal efficiency and reusability (Figure 8).

6. Proposed adsorption mechanism of Hg^{2+} adsorption

The Mercury (Hg^{2+}) was successfully confiscated from water on adsorbing surface of graphene oxide-metal organic framework (ZIF-67@GO) due to the availability of inner pores of the surfaces of adsorbent. Adsorption process was reinforced because of high surface area of composite (adsorbent) pores as compared to adsorbate. Results of the kinetic models applied have shown that Reported literature indicated that ZIF-67 with a zeta potential of 6.5 has strong surfaces to trap Hg^{2+} molecules into ZIF-67@GO pores from aqueous media. Some important features like surface (hydrophobic) and electrostatic interaction played their role in mercury (Hg^{2+}) confiscation. The correlation coefficients Values (R^2) for applied models to study adsorption study were also determined. After satisfactory results, it was observed that multilayer chemisorption process/mechanism is elaborate during whole processes for Hg^{2+} confiscation via adsorption on ZIF-67@GO composite because of the presence of fine sheets of graphene oxide and highly functional active cites of MOF which was successfully deposited on GO surface. It has already reported that such type of adsorption depends on different

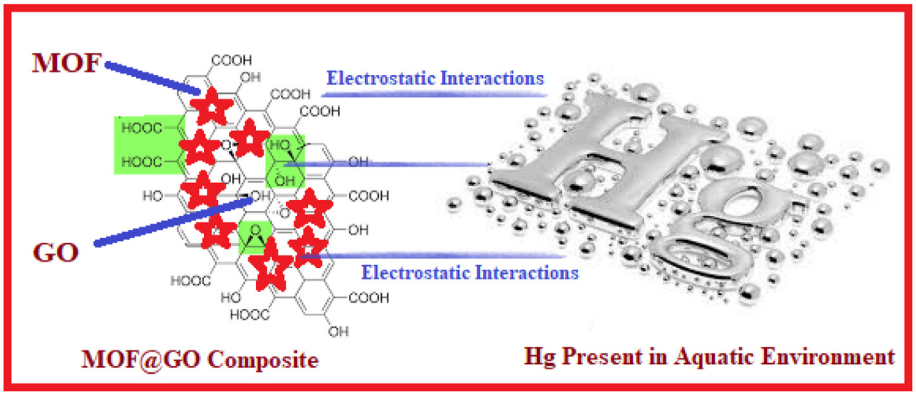

Figure 9. Proposed adsorption Mechanism for Hg^{2+} clearly indication the adsorption through electrostatic and π-π interaction between ZIF-67@GO composite and Hg^{2+}.

groups of adsorbents surfaces. This provided strongest evidence that our material was successfully synthesized and it has the capacity to adsorb Hg^{2+} due to electrostatic interaction between the ZIF-67@GO and Hg^{2+} on ZIF-67@GO surface. After adsorption the EDX analysis were carried out to confirm the adsorption of Hg^{2+} on the surface of composite. The EDX Results provided evidence for Hg^{2+} adsorption by MOF@GO composites (Figure S6). It was found during subsequently adsorption experiment that hydrophobicity became troublesome which results in a higher-degree disorder of bulk structure of H_2O. Projected mechanism of Hg^{2+} confiscation using ZIF-67@GO is shown in Figure 9.

7. Conclusion

This study was aimed at confiscation of mercury (Hg^{+2}) from aqueous media using ZIF-67@GO, prepared using solvothermal method of synthesis. The synthesized compounds were confirmed using FTIR, SEM, EDX and XRD. The adsorption experiment was monitored by atomic adsorption spectroscopy. The prepared ZIF-67@GO were tested as adsorbent for Hg^{2+} confiscation and adsorption experiments results revealed that it is efficient for Hg^{2+} confiscation. The maximum removal efficiency was 91.1% using 10 mg of prepared adsorbent material. Effects of pH, Hg^{2+} concentration, contact time, adsorption kinetics were also studied. Results showed that adsorption study fitted well to Freundlich isotherm with R^2 value of 0.9925 than that of Langmuir isotherm with R^2 value of 0.9238). Kinetics models of adsorption was rapid and best fitted for pseudo 2nd order ($R^2 = 0.99946$) than 1st order model ($R^2 = 0.8836$), which indicated that multilayer chemisorption occurs during adsorption process. The highly water stable ZIF-67@GO composites have revealed excellent reusability after many cycles indicating excellent reusability, high thermal and water stability of the graphene-oxide metal organic framework composite (ZIF-67@GO). Consequently, it can be said that prepared ZIF-67@GO composite can efficiently be used for confiscation of Hg^{2+} from water.

Declarations

Author contribution statement

Ahmed M. Fallatah: Performed the experiments.

Habib Ur Rehman Shah: Analyzed and interpreted the data; Wrote the paper.

Khalil Ahmad: Performed the experiments; Analyzed and interpreted the data.

Muhammad Ashfaq; Abdul Rauf: Conceived and designed the experiments.

Muhammad Muneer; Zeinhom M. El-Bahy: Contributed reagents, materials, analysis tools or data.

Mohamed M. Ibrahim; Afshain Babras: Analyzed and interpreted the data.

Amir Shahzad: Wrote the paper; Contributed reagents materials, analysis tools or data.

Funding statement

This work was supported by Taif Researchers Supporting project [TURSP-2020/46].

Data availability statement

Data included in article/supplementary material/referenced in article.

Declaration of interest's statement

The authors declare no conflict of interest.

Additional information

Supplementary content related to this article has been published online at https://doi.org/10.1016/j.heliyon.2022.e10936.

Acknowledgements

Authors are thankful to the Institute of chemistry, Baghdad Ul Jadeed Campus, The Islamia University of Bahawalpur, Punjab, Pakistan for providing necessary facilities to complete present research project. This work was supported by Taif Researchers Supporting Project (TURSP-2020/46), Taif University, Taif, Saudi Arabia.

References

[1] M.A. Nazir, et al., Quality assessment of the noncarbonated-bottled drinking water: comparison of their treatment techniques, Int. J. Environ. Anal. Chem. (2020) 1–12.
[2] C.A. Graves, et al., Marine water quality of a densely populated Pacific atoll (Tarawa, Kiribati): cumulative pressures and resulting impacts on ecosystem and human health, Mar. Pollut. Bull. 163 (2021), 111951.
[3] R.P. Schwarzenbach, et al., The challenge of micropollutants in aquatic systems, Science 313 (5790) (2006) 1072–1077.
[4] M. Urbina, et al., A country's response to tackling plastic pollution in aquatic ecosystems: the Chilean way, Aquat. Conserv. Mar. Freshw. Ecosyst. 31 (2) (2021) 420–440.
[5] K. Ahmad, et al., Effect of metal atom in zeolitic imidazolate frameworks (ZIF-8 & 67) for removal of Pb^{2+} & Hg^{2+} from water, Food Chem. Toxicol. 149 (2021), 112008.
[6] M.A. Bradley, B.D. Barst, N. Basu, A review of mercury bioavailability in humans and fish, Int. J. Environ. Res. Publ. Health 14 (2) (2017) 169.
[7] S. Zhao, et al., A review on mercury in coal combustion process: content and occurrence forms in coal, transformation, sampling methods, emission and control technologies, Prog. Energy Combust. Sci. 73 (2019) 26–64.
[8] P.O. Ozuah, Mercury poisoning, Curr. Probl. Pediatr. 30 (3) (2000) 91–99.
[9] V. Gupta, P. Singh, N. Rahman, Adsorption behavior of Hg (II), Pb (II), and Cd (II) from aqueous solution on Duolite C-433: a synthetic resin, J. Colloid Interface Sci. 275 (2) (2004) 398–402.
[10] D.L. Haskins, et al., Brown watersnakes (Nerodia taxispilota) as bioindicators of mercury contamination in a riverine system, Sci. Total Environ. 755 (2021), 142545.
[11] N. Rahman, P. Varshney, M. Nasir, Synthesis and characterization of polydopamine/hydrous zirconium oxide composite and its efficiency for the removal of uranium (VI) from water, Environ. Nanotechnol. Monit. Manag. 15 (2021), 100458.
[12] N. Rahman, et al., Synthesis of 2-mercaptopropionic acid/hydrous zirconium oxide composite and its application for removal of Pb (II) from water samples: central composite design for optimization, J. King Saud Univ. Sci. 33 (2) (2021), 101280.
[13] N. Rahman, et al., Efficient removal of Pb (II) from water using silica gel functionalized with thiosalicylic acid: response surface methodology for optimization, J. King Saud Univ. Sci. 33 (1) (2021), 101232.
[14] N. Rahman, M. Nasir, Facile synthesis of thiosalicylic acid functionalized silica gel for effective removal of Cr (III): equilibrium modeling, kinetic and thermodynamic studies, Environ. Nanotechnol. Monit. Manag. 14 (2020), 100353.
[15] R.D. Behrooz, G. Poma, Evaluation of mercury contamination in Iranian wild cats through hair analysis, Biol. Trace Elem. Res. 199 (1) (2021) 166–172.
[16] K. Ahmad, et al., Synthesis and spectroscopic characterization of medicinal azo derivatives and metal complexes of Indandion, J. Mol. Struct. 1198 (2019), 126885.
[17] M.E. Crespo-Lopez, et al., Mercury: what can we learn from the Amazon? Environ. Int. 146 (2021), 106223.
[18] J.P. Novo, et al., Cellular and molecular mechanisms mediating methylmercury neurotoxicity and neuroinflammation, Int. J. Mol. Sci. 22 (6) (2021) 3101.
[19] G. Guzzi, A. Ronchi, P. Pigatto, Toxic effects of mercury in humans and mammals, Chemosphere 263 (2021), 127990.
[20] K.J. Lee, Development of Reporting Guidelines for Systematic Review for Environmental Epidemiology Studies, Université d'Ottawa/University of Ottawa, 2021.
[21] Y. Miyamoto, A World Otherwise: Environmental Praxis in Minamata, Lexington Books, 2021.
[22] S. Ekino, et al., Minamata disease revisited: an update on the acute and chronic manifestations of methyl mercury poisoning, J. Neurol. Sci. 262 (1-2) (2007) 131–144.
[23] G. Zhu, et al., Application of Fe-MOFs in advanced oxidation processes, Res. Chem. Intermed. 45 (7) (2019) 3777–3793.
[24] N. Rahman, M. Nasir, Facile synthesis of thiosalicylic acid functionalized silica gel for effective removal of Cr(III): equilibrium modeling, kinetic and thermodynamic studies, Environ. Nanotechnol. Monit. Manag. 14 (2020), 100353.
[25] N. Rahman, et al., Efficient removal of Pb(II) from water using silica gel functionalized with thiosalicylic acid: response surface methodology for optimization, J. King Saud Univ. Sci. 33 (1) (2021), 101232.
[26] N. Rahman, et al., Synthesis of 2-mercaptopropionic acid/hydrous zirconium oxide composite and its application for removal of Pb(II) from water samples: central composite design for optimization, J. King Saud Univ. Sci. 33 (2) (2021), 101280.

[27] V.K. Gupta, P. Singh, N. Rahman, Adsorption behavior of Hg(II), Pb(II), and Cd(II) from aqueous solution on Duolite C-433: a synthetic resin, J. Colloid Interface Sci. 275 (2) (2004) 398–402.

[28] L. Guzzella, D. Feretti, S. Monarca, Advanced oxidation and adsorption technologies for organic micropollutant removal from lake water used as drinking-water supply, Water Res. 36 (17) (2002) 4307–4318.

[29] M.A. Nazir, et al., Combining structurally ordered intermetallic nodes: kinetic and isothermal studies for removal of malachite green and methyl orange with mechanistic aspects, Microchem. J. 164 (2021), 105973.

[30] M.A. Nazir, et al., Synthesis of porous secondary metal-doped MOFs for removal of Rhodamine B from water: role of secondary metal on efficiency and kinetics, Surface. Interfac. 25 (2021), 101261.

[31] M.A. Nazir, et al., Surface induced growth of ZIF-67 at Co-layered double hydroxide: removal of methylene blue and methyl orange from water, Appl. Clay Sci. 190 (2020), 105564.

[32] C.S. Kim, et al., Mercury speciation by X-ray absorption fine structure spectroscopy and sequential chemical extractions: a comparison of speciation methods, Environ. Sci. Technol. 37 (22) (2003) 5102–5108.

[33] J.F. Risher, S.N. Amler, Mercury exposure: evaluation and intervention: the inappropriate use of chelating agents in the diagnosis and treatment of putative mercury poisoning, Neurotoxicology 26 (4) (2005) 691–699.

[34] K. Ahmad, et al., Lead in drinking water: adsorption method and role of zeolitic imidazolate frameworks for its remediation: a review, J. Clean. Prod. (2022), 133010.

[35] Ahmed, K.N., et al., Comparative Study between Two Zeolitic Imidazolate Frameworks as Adsorbents for Removal of Organoarsenic, as (III) and as (V) Species from Water.

[36] H.-U.R. Shah, et al., Metal organic frameworks for efficient catalytic conversion of CO_2 and CO into applied products, Mol. Catal. 517 (2022), 112055.

[37] K. Ahmad, et al., Synthesis and characterization of water stable polymeric metallo organic composite (PMOC) for the removal of arsenic and lead from brackish water, Toxin Rev. 41 (2) (2022) 577–587.

[38] K. Ahmad, et al., Effect of metal atom in zeolitic imidazolate frameworks (ZIF-8 & 67) for removal of Pb^{2+} & Hg^{2+} from water, Food Chem. Toxicol. 149 (2021), 112008.

[39] H.A. Naseem, et al., Rational synthesis and characterization of medicinal phenyl diazenyl-3-hydroxy-1h-inden-1-one azo derivatives and their metal complexes, J. Mol. Struct. 1227 (2021), 129574.

[40] H.U.R. Shah, et al., Synthetic routes of azo derivatives: a brief overview, J. Mol. Struct. 1244 (2021), 131181.

[41] J.B. Pan, et al., Activity and stability boosting of an oxygen-vacancy-rich $BiVO_4$ photoanode by NiFe-MOFs thin layer for water oxidation, Angew. Chem. 133 (3) (2021) 1453–1460.

[42] T. Najam, et al., Nanostructure engineering by surficial induced approach: porous metal oxide-carbon nanotube composite for lithium-ion battery, Mater. Sci. Eng., B 273 (2021), 115417.

[43] S.S.A. Shah, et al., Surface engineering of MOF-derived FeCo/NC core-shell nanostructures to enhance alkaline water-splitting, Int. J. Hydrogen Energy 47 (8) (2022) 5036–5043.

[44] N.A. Khan, et al., Efficient removal of norfloxacin by MOF@ GO composite: isothermal, kinetic, statistical, and mechanistic study, Toxin Rev. 40 (4) (2021) 915–927.

[45] M.K. Aslam, et al., Kinetically controlled synthesis of MOF nanostructures: single-holed hollow core–shell ZnCoS@ Co 9 S 8/NC for ultra-high performance lithium-ion batteries, J. Mater. Chem. 6 (29) (2018) 14083–14090.

[46] T. Najam, et al., Role of P-doping in antipoisoning: efficient MOF-derived 3D hierarchical architectures for the oxygen reduction reaction, J. Phys. Chem. C 123 (27) (2019) 16796–16803.

[47] Z. Zhang, et al., Molecular study of heterogeneous mercury conversion mechanism over Cu-MOFs: oxidation pathway and effect of halogen, Fuel 290 (2021), 120030.

[48] P. Horcajada, et al., Porous metal–organic-framework nanoscale carriers as a potential platform for drug delivery and imaging, Nat. Mater. 9 (2) (2010) 172–178.

[49] O.P. Kumar, et al., Strategic combination of metal–organic frameworks and C_3N_4 for expeditious photocatalytic degradation of dye pollutants, Environ. Sci. Pollut. Control Ser. 29 (23) (2022) 35300–35313.

[50] M.A. Nazir, et al., Enhanced adsorption removal of methyl orange from water by porous bimetallic Ni/Co MOF composite: a systematic study of adsorption kinetics, Int. J. Environ. Anal. Chem. (2021) 1–16.

[51] L. Huang, et al., Facile fabrication of N-doped magnetic porous carbon for highly efficient mercury removal, ACS Sustain. Chem. Eng. 6 (8) (2018) 10191–10199.

[52] M. Li, et al., Fabrication of Fe_3O_4/ZIF-67 composite for removal of direct blue 80 from water, Water Environ. Res. 92 (5) (2020) 740–748.

[53] T.H. Lee, et al., Elucidating the role of embedded metal–organic frameworks in water and ion transport properties in polymer nanocomposite membranes, Chem. Mater. 32 (23) (2020) 10165–10175. In press.

[54] S.S.A. Shah, et al., Effect of metal atom in zeolitic imidazolate frameworks (ZIF-8 & 67) for removal of Pb^{2+} & Hg, Food Chem. Toxicol. 149 (2021), 112008.

[55] W.S. Hummers Jr., R.E. Offeman, Preparation of graphitic oxide, J. Am. Chem. Soc. 80 (6) (1958) 1339.

[56] H.U.R. Shah, et al., Water stable graphene oxide metal-organic frameworks composite (ZIF-67@ GO) for efficient removal of malachite green from water, Food Chem. Toxicol. (2021), 112312.

[57] C. Liang, et al., ZIF-67 derived hollow cobalt sulfide as superior adsorbent for effective adsorption removal of ciprofloxacin antibiotics, Chem. Eng. J. 344 (2018) 95–104.

[58] S. Kumari, et al., Efficient and highly selective adsorption of cationic dyes and removal of ciprofloxacin antibiotic by surface modified nickel sulfide nanomaterials: kinetics, isotherm and adsorption mechanism, Colloids Surf. A Physicochem. Eng. Asp. 586 (2020), 124264.

[59] N. Rahman, A. Raheem, Graphene oxide/Mg-Zn-Al layered double hydroxide for efficient removal of doxycycline from water: taguchi approach for optimization, J. Mol. Liq. 354 (2022), 118899.

[60] V.M. Yau, et al., Prenatal and neonatal peripheral blood mercury levels and autism spectrum disorders, Environ. Res. 133 (2014) 294–303.

[61] O. Miura, S. Tachibana, Mercury removal from solution by high gradient magnetic separation with functional group modified magnetic activated carbon, IEEE Trans. Appl. Supercond. 24 (3) (2013) 1–4.

[62] M.J. Shadbad, A. Mohebbi, A. Soltani, Mercury (II) removal from aqueous solutions by adsorption on multi-walled carbon nanotubes, Kor. J. Chem. Eng. 28 (4) (2011) 1029–1034.

[63] H. Parham, B. Zargar, R. Shiralipour, Fast and efficient removal of mercury from water samples using magnetic iron oxide nanoparticles modified with 2-mercaptobenzothiazole, J. Hazard Mater. 205 (2012) 94–100.

[64] T. Okamoto, et al., Mercury removal from solution by superconducting magnetic separation with nanostructured magnetic adsorbents, Phys. C: Supercond. Appl. 471 (21-22) (2011) 1516–1519.

[65] S. Thakur, et al., A new guar gum-based adsorbent for the removal of Hg (II) from its aqueous solutions, Carbohydr. Polym. 106 (2014) 276–282.

[66] W. Wang, et al., Thiol-rich polyhedral oligomeric silsesquioxane as a novel adsorbent for mercury adsorption and speciation, Chem. Eng. J. 242 (2014) 62–68.

[67] J. Zhou, et al., CeO_2–TiO_2 sorbents for the removal of elemental mercury from syngas, Environ. Sci. Technol. 47 (17) (2013) 10056–10062.

[68] N. Asasian, T. Kaghazchi, M. Soleimani, Elimination of mercury by adsorption onto activated carbon prepared from the biomass material, J. Ind. Eng. Chem. 18 (1) (2012) 283–289.

[69] J.-G. Yu, et al., Removal of mercury by adsorption: a review, Environ. Sci. Pollut. Control Ser. 23 (6) (2016) 5056–5076.

[70] J.M. Arsuaga, et al., Aqueous mercury adsorption in a fixed bed column of thiol functionalized mesoporous silica, Adsorption 20 (2-3) (2014) 311–319.

[71] K. Johari, N. Saman, H. Mat, A comparative evaluation of mercury (II) adsorption equilibrium and kinetics onto silica gel and sulfur-functionalised silica gels adsorbents, Can. J. Chem. Eng. 92 (6) (2014) 1048–1058.

[72] H. Cui, et al., Fast removal of Hg (II) ions from aqueous solution by amine-modified attapulgite, Appl. Clay Sci. 72 (2013) 84–90.